An Optical Vortex Coronagraph

David M. Palacios

Jet Propulsion Laboratory

California Institute of Technology

4800 Oak Grove Dr., Pasadena, CA 91109

David.M.Palacios@jpl.nasa.gov

ABSTRACT

An optical vortex may be characterized as a dark core of destructive interference in a beam of spatially coherent light. This dark core may be used as a filter to attenuate a coherent beam of light so an incoherent background signal may be detected. Applications of such a filter include: eye and sensor protection, forward-scattered light measurement, and the detection of extra-solar planets. Optical vortices may be created by passing a beam of light through a vortex diffractive optical element, which is a plate of glass etched with a spiral pattern, such that the thickness of the glass increases in the azimuthal direction. An optical vortex coronagraph may be constructed by placing a vortex diffractive optical element near the image plane of a telescope. An optical vortex coronagraph opens a dark window in the glare of a distant star so nearby terrestrial sized planets and exo-zodiacal dust may be detected. An optical vortex coronagraph may hold several advantages over other techniques presently being developed for high contrast imaging, such as lower aberration sensitivity and multi-wavelength operation. In this manuscript, I will discuss the aberration sensitivity of an optical vortex coronagraph and the key advantages it may hold over other coronagraph architectures. I will also provide numerical simulations demonstrating high contrast imaging in the presence of low-order static aberrations.

Keywords: coronagraphs; terrestrial planets; optical vortices;

1. INTRODUCTION

The Terrestrial Planet Finder Coronagraph is a proposed space telescope designed to greatly enhance the contrast between a terrestrial planet and its host star in visible light (500-800nm). The TPF coronagraph is required[1] to provide at least 10^{-10} starlight suppression with a stability of $2.5\text{x}10^{-11}$ at an inner working angle of $4\lambda/D$ where D is the longest dimension of the primary mirror* and λ_0=550nm is the telescopes optimal operating wavelength.

In order to meet these tight requirements several coronagraph designs have been studied[2,3,4]. Presently, Band-limited masks have shown the greatest starlight suppression[5]. Trauger[6] et al has demonstrated monochromatic light

* The primary mirror is designed to have an elliptical shape with the major axis equal to 8m and the minor axis equal to 3.5m.

suppression on the order of (~10^{-9}) by using a linear-sinc^2 mask in conjunction with wave-front control on the High Contrast Imaging Test Bed (HCIT) at JPL. However, the most successful band-limited mask used on HCIT (a linear sinc^2 mask) was designed for an operating wavelength, λ_0=800nm. Broadband operation between 500-800nm has not yet been demonstrated. Nor have the masks been fabricated to operate at the shorter wavelength requirement of 500nm.

A new type of band-limited mask known as an 8th order mask is presently under examination for its relative insensitivity to low order aberrations. The linear Sinc^2 masks that have demonstrated (~1e^{-9}) light suppression on HCIT belong to a family of occulting masks known as 4th order masks. Named thusly because the intensity of the residual light, post coronagraph, exhibits a 4th order dependence to a tilt/tip aberration. Kucher[7] et al devised a way to create a mask with an 8th order sensitivity to tip/tilt by combining two properly weighted and arranged linear sinc^2 functions. However, this comes at the price of reduced planet light throughput in comparison to the starlight throughput. The high contrast performance of these masks is currently under investigation on HCIT at JPL.

In this paper I will examine a new type of coronagraph occulting mask known as an optical vortex diffractive optical element (vortex mask). These masks produce phase defects with dark central spots where the light from an on-axis star is ideally reduced to zero, opening a window within the star where nearby terrestrial sized planets and exo-zodiacal dust may be detected[8]. By using a simple theoretical model, I will examine how a vortex coronagraph may be constructed to possess a 10th order aberration sensitivity yet still obtain a throughput comparable to an 8th order mask. Optical vortex masks have already demonstrated low contrast (~10^{-5}) light suppression[9] as well as simultaneous operation at wavelengths ranging from 425-850nm[10]. In this paper I will discuss how optical vortex masks may be used to obtain high contrast starlight suppression (~10^{-10}) at several wavelengths simultaneously.

Vortices are ubiquitous features of waves in nature. They are known to occur in many physical systems[11,12,13], such as fluids, Bose-Einstein condensates , superconductors , super-fluid helium, and light. An optical vortex may be characterized as a dark core of destructive interference in a beam of spatially coherent light. This dark core may be used as a filter to attenuate a coherent beam of light so a mutually incoherent background signal may be detected[8]. A single optical vortex in the center of a scalar monochromatic beam propagating in the z direction may be written in cylindrical coordinates (ρ, ϕ, z)[13]:

$$E(\rho,\ \phi,\ z,\ t) = A(\rho,\ z)\exp(im\phi)\exp(i\omega t - ikz) \tag{1}$$

where $A(\rho, z)$ is a circularly symmetric amplitude function, k=2π/λ is the wave number of a monochromatic field of wavelength λ, and m is a signed integer known as the topological charge. The vortex nature of the field is governed by the phase factor, $exp(im\phi)$. At a fixed instant of time helical surfaces of constant phase given by $m\phi - kz$=const are produced for integer values of m. The amplitude vanishes along the helix axis (ρ=0) owing to destructive interference in the vicinity of the vortex core i.e., $A(0, z)$=0. The topological charge of a defect may be calculated using the line integral[13]:

$$m = (1/2\pi)\oint \nabla\phi\, ds \tag{2}$$

where $\nabla\phi$ is the gradient of the phase and ds is a line enclosing the defect. The amplitude and phase of an m=1 vortex is depicted in Fig. 1. A monochromatic, planar (m=0) beam can be converted into a vortex beam by transmitting the light through a transparent diffractive phase mask having a thickness given by[14],

$$d = d_0 - m\lambda_0\phi/2\pi(n_s - n_0) \quad (3)$$

where d_0 is the nominal thickness, λ_0 is the wavelength for which the mask is intended, n_s is the refractive index of the substrate, and n_0 is the index of refraction of the surrounding medium. Light passing through the mask gains an azimuthally varying phase and an amplitude profile with a dark core embedded within it.

2. CORONAGRAPH ARCHITECTURE

A simple unfolded architecture of a vortex coronagraph is depicted in Fig. 2. Light from a distant star is imaged by L_1, which represents the telescope optics. A vortex mask is placed near the focus to create a dark central null in the beam. A collimator represented by L_2 collimates the beam after the starlight passes through the vortex mask. In the collimated space between L_1 and L_2 a circular Lyot stop blocks the unwanted starlight thereby allowing the enhanced detection of nearby objects. The remaining light is then re-imaged by L_3 with the on-axis starlight greatly attenuated compared to the off-axis light from the planet.

In this paper, I will assume circular instead of elliptical symmetry since the present TPF mission design contains beam-circularizing optics to increase the efficacy of the wave-front control system. In a circularly symmetric system, the dark null created by the vortex phase mask will also have circular symmetry as shown in Fig. 1, therefore the optimal Lyot stop is a circular aperture.

3. ABERRATION SENSITIVITY

One metric of coronagraph system performance of vital importance to TPF is the contrast sensitivity of the system to low-order aberrations. Presently 8th order masks have demonstrated the lowest theoretical aberration sensitivity[15]. They are so named because they are not sensitive to aberrations that contribute to the first three terms in the Taylor's expansion of the exit pupil. Thus they are sensitive to aberrations that have a 4th order dependence in amplitude or 8th order dependence in intensity. By comparison the best light suppression demonstrated on HCIT was performed with a linear sinc^2 mask, which has a 4th order aberration sensitivity in intensity.

In this section, I will show that an optical vortex mask will theoretically have a 2mth order aberration sensitivity in intensity. Therefore an m=4 mask will theoretically produce the same aberration sensitivity of the 8th order masks and higher charged vortex masks will be even less sensitive to aberrations. Throughout this paper I will assume an m=5 vortex mask designed for λ_0=550nm, because manufacturing such a mask should be possible with present day ion beam lithography techniques.

As I stated previously, when light is transmitted through a vortex mask it gains an azimuthal phase ramp and the amplitude of the field vanishes at the center of the ramp (ρ=0) owing to destructive interference in the vicinity of the core. The amplitude transmission function of a vortex mask may be approximated as[16]:

$$M(\rho) = \tanh^m(\rho/w_v) \quad (4)$$

Where w_v is a fitting parameter which describes the vortex core size. For an ideal point vortex, which is strictly non-physical, $w_v \to 0$. Also as the vortex propagates from the mask the value of w_v will also increase due to diffraction[17]. By expanding Eq.(4) in a Taylor's series about ρ=0 the mask transmission function my be represented by a polynomial series:

$$M(\rho) \approx \sum_{k=1,2,3...} a_k \rho^k \tag{5}$$

Where the a_k values are given by,

$$a_k = \frac{1}{w_v k!} \frac{\partial^k}{\partial \rho^k} M(\rho = 0) \tag{6}$$

A close examination of a_k using $M(\rho)$ defined in Eq.(4) reveals that the derivatives of the mask transmission function disappear for all the terms in the expansion up to the m[th] term.

Now let us consider light at the entrance pupil of the coronagraph. Assuming the pupil has an amplitude transmission function, $P(r)$, and a phase transmission function $\Theta(r,\theta)$ <<1, then the complex field at the pupil may be represented as:

$$E(r,\theta) = P(r)\left(1 + \sum_{l=1,2,3...} \frac{i^l}{l!} \Phi^l(r,\theta)\right) \tag{7}$$

Where $P(r)$=1 inside the pupil and $P(r)$=0 outside of the pupil. The telescope optics (represented by L1 in Fig. 2) form an image at the focus of L1 after the starlight is first transmitted through a vortex mask placed near the focus of L1. The field at the focus of L1 may then be represented as:

$$E(\rho,\phi) = FT\{E(r,\theta)\} \cdot M(\rho)\exp(im\phi) \tag{8}$$

where FT{} denotes a two-dimensional Fourier Transform. As shown in Fig. 2**,** Lens L2 collimates the beam of light passing through the occulting mask forming an image of the pupil. The re-imaged pupil, $P_{exit}(r,\theta)$ may be represented by the convolution:

$$P_{exit}(r,\theta) = E(r,\theta) * FT\{M(\rho)\exp(im\phi)\} \tag{9}$$

where (*) represents a convolution operation. The $FT\{M(\rho)exp(im\phi)\}$ may be represented by a Hankel transform of $M(\rho)$ of order m[16]. By using Eq. (5) we may represent $FT\{M(\rho)exp(im\phi)\}$ as :

$$FT\{M(\rho)\exp(im\phi)\} = H_m\{M(\rho)\} = \sum_{k=m,\,m+1,\,m+2...} a_k H_m\{\rho^k\} \tag{10}$$

where $H_m\{f(\rho)\}$ represents the m[th] order Hankel transform of $f(\rho)$. Using the identity[18]:

$$H_m\{\rho^k f(\rho)\} = \left(\frac{-1}{2\pi}\right)^k r^{m-k} \frac{d^k}{dr^k}\left[\frac{1}{r^{m-k}} H_{m-k}\{f(\rho)\}\right] \tag{11}$$

as well as Eq. (7), $P_{exit}(r,\theta)$ may be represented as:

$$P_{exit}(r,\theta) = P(r)\left(1 + \sum_{l=1,2,3...} \frac{i^l}{l!} \Phi^l(r,\theta)\right) * \sum_{k=m,m+1,m+2...} a_k \left(\frac{-1}{2\pi}\right)^k r^{m-k} \frac{d^k}{dr^k}\left[\frac{1}{r^{m-k}} \delta(r)\right] \tag{12}$$

Examination of the first term (k=m) in the mask transmission function expansion reveals:

$$P_{exit}(r,\theta) \approx a_m \left(\frac{-1}{2\pi}\right)^m \frac{d^m}{dr^m}\left[P(r)\left(1+\sum_{l=1,2,3\ldots}\frac{i^l}{l!}\Phi^l(r,\theta)\right)\right] \tag{13}$$

Consider now, the first term in the expansion of the phase aberration *(l=1)* in Eq. (13). The Leakage through the pupil to this term is the m^{th} derivative of the phase aberration and will vanish for any phase aberration with a radial dependence less than m. Therefore the coronagraph will exhibit an m^{th} order aberration sensitivity in amplitude and a $2m^{th}$ sensitivity in intensity. In the next section I will provide numerical simulations of the aberration sensitivity of an m=5 vortex mask.

4. NUMERICAL SIMULATIONS

The performance of an optical vortex coronagraph was simulated with an ideal imaging system possessing the following parameters:

- All simulations were performed on a 1024x1024 grid array.
- The vortex mask was designed to produce an m=5 vortex at λ= 550nm.
- The entrance pupil diameter, D=1000 pixels.
- The Lyot diameter, D_L= 0.52D.
- The amplitude transmission function of the mask had a form given by Eq. (4) with w_v=0.014D. This was chosen to reduce numerical noise caused by the discontinuity at the origin, while yet not affecting the value of contrast at the inner working angle of 4λ/D.
- The focal plane profile of lens L1 in Fig. 2 was assumed to be an ideal Somb(r) function before application of the vortex mask.

Contrast as defined by Green[19] et al was used as a metric of system performance. The contrast was computed by measuring the final focal plane intensity with and without a vortex mask present at the focus of L1. The first 12 Noll ordered Zernike aberrations[20] were applied to the entrance pupil of the system (located at L1 in Fig. 2). Figure 3 is a plot of the contrast vs. peak to valley aberration level for several of the low-order Zernike Aberrations. The contrast sensitivity of the vortex coronagraph was determined by a least squares fit of the contrast plots depicted in Fig. 3 to a power law given by:

$$C = \alpha + \beta\rho^{\gamma} \tag{14}$$

where α is the residual contrast when no aberrations are present (of order ~10^{-16}), β is a scaling factor determined from the least squares fit, and γ is the power law exponent. The values of γ for each low-order Zernike are listed in Table 1 as well as the values obtained by Shaklan[15] et al. According to the values of g given for tip/tilt (z=2, z=3) the m=5 vortex coronagraph did not obtain the ideal 10^{th} order behavior predicted in the previous section but did demonstrate 9^{th} order behavior. This departure from ideal is most likely due to the addition of higher order terms in the mask expansion. Regardless of this small discrepancy, the m=5 vortex coronagraph did demonstrate a lower aberration sensitivity than a linear 8^{th} order mask. It should also be noted that the optical vortex coronagraph throughput for a planet located at a

radial position of 4λ/D was equal to the throughput for the optimized 8th order coronagraph Shaklan[15] et al. simulated. Interestingly, not only is the vortex coronagraph less sensitive to low-order aberrations, it appears to obtain a much lower contrast floor with the same throughput. However, the simulations reported by Shaklan[15] et al had a much higher noise floor (~10^{-13}), which may account for the difference. A side-by-side comparison of the vortex coronagraph and an 8th order coronagraph is presently under investigation.

5. MULTI-WAVELENGTH OPERATION

To meet the needs of the TPF mission, the starlight suppression system must be able to operate over a broad spectral range (500-800 nm)*. The starlight suppression systems presently under investigation do not appear to satisfactorily meet this requirement. One possible advantage an optical vortex coronagraph may have for the TPF mission is its ability to operate at several wavelengths simultaneously. Vortex phase masks are optimally made for one wavelength by etching a spiral into a glass substrate such as fused silica glass. However, a vortex will also form at other wavelengths that have an integer topological charge. For instance, by using Eq. (3) and assuming the glass used is non-dispersive, we can see that a vortex mask designed to produce an m=5 vortex at 550nm will also form an m=4 vortex at 688nm, an m=3 vortex at 916nm, and an m=2 vortex at 1375nm. By changing the topological charge the aberration sensitivity will increase, but at the longer wavelengths the aberrations will have a smaller effect on the wave front. An m=1 vortex mask designed for 850nm has already demonstrated operation over a wavelength range between 425nm and 850nm[10]. Broadband vortex coronagraph operation is presently under investigation.

6. CLOSING REMARKS

An optical vortex coronagraph may hold several key advantages for the TPF mission than other coronagraph occulting masks. These advantages include lower aberration sensitivity and multi-wavelength operation. Also since the coronagraph is relatively insensitive to small aberrations it may be possible to increase the Lyot stop size, thereby increasing the overall throughput of the system. Vortex masks with topological charge ranging from m=1-3 have been previously manufactured. Using present ion-beam lithography techniques, it should be possible to construct an m=5 vortex mask designed for an optical wavelength of λ_0=550nm.

ACKNOWLEDGMENTS

I'd like to thank G.A. Swartzlander Jr. for many helpful discussions on optical vortices. I would also like to thank S. Shaklan and J. Green for their suggestions and comments.

* There has even been discussion of broadening this range further to (500-1500nm), to increase our ability to characterize the detected planets.

REFERENCES

[1] Ford, V.G., et al 2004, Proc. SPIE 5487, 1274

[2] Kasdin, N.J., Vanderbei, R.J. Spergel, D.N., and Littman, M.G. 2003, ApJ, 582, 1147

[3] Guyon, O. 2003, A&A, 404, 379

[4] Rouan, D., Bocceletti, A. Riaud, P., and Baudrand, J. 2003 Proc. SPIE 4860, 192

[5] Kuchner, M.J., and Traub, W.A. 2002, ApJ, 570, 900

[6] Trauger, J.T. et al 2004, Proc. SPIE 5487, 1330

[7] Kuchner, M.J., Crepp, J., and Ge, J. 2004, APJ, (astro-ph/0411077)

[8] G.A. Swartzlander Jr., Opt. Lett. **26**, 497 (2001).

[9] David Palacios, David Rozas, and Grover A. Swartzlander Jr., Phys. Rev. Lett. **88**, art. # 103902 (2002).

[10] David M. Palacios, "An Optical Vortex Coherence Filter", Ph.D. Dissertation at the Worcester Polytechnic Institute (2004). (http://www.wpi.edu/Pubs/ETD/Available/etd-0824104-123434/)

[11] L.M. Pismen, *Vortices in Nonlinear Field*s, Oxford Science Publications (Clarendon Press, Oxford, 1999).

[12] Sheldon Green eds., *Fluid Vortices*, (Kluwer Academic Publishers, Dordrecht, Netherlands, 1995).

[13] M. Vasnetsov and K. Staliunas, eds., *Optical Vortices*, vol. 228, Horizons in World Physics, (Nova Science, Huntington, NY, 1999).

[14] F.B. Colstoun, G. Khitrova, A.V. Fedorov, T.R. Nelson, C. Lowery, T.M. Brennan, B.G. Hammons, and P.D. Maker, Chaos, Solitons, & Fractals **4**, 1575-1596 (1995).

[15] Shaklan, S.B., and Green, J.J, accepted to ApJ 2005.

[16] Trillo, S. & Torruellas, W. (eds) *Spatial Solitons* (Springer, Berlin, 2001)

[17] Z.S. Sacks, D. Rozas, and G.A. Swartzlander, Jr., J.Opt. Soc. Am. B **15**, 2226-2234 (1998).

[18] Gaskill, J.D. 1978, Linear Systems, Fourier Transforms, and Optics, (New York: John Wiley & Sons) pg 320.

[19] Green, J.J., and Shaklan, S.B. 2003, Proc. SPIE 5170, 25

[20] Noll, R.J., 1976, JOSA, 66, 207

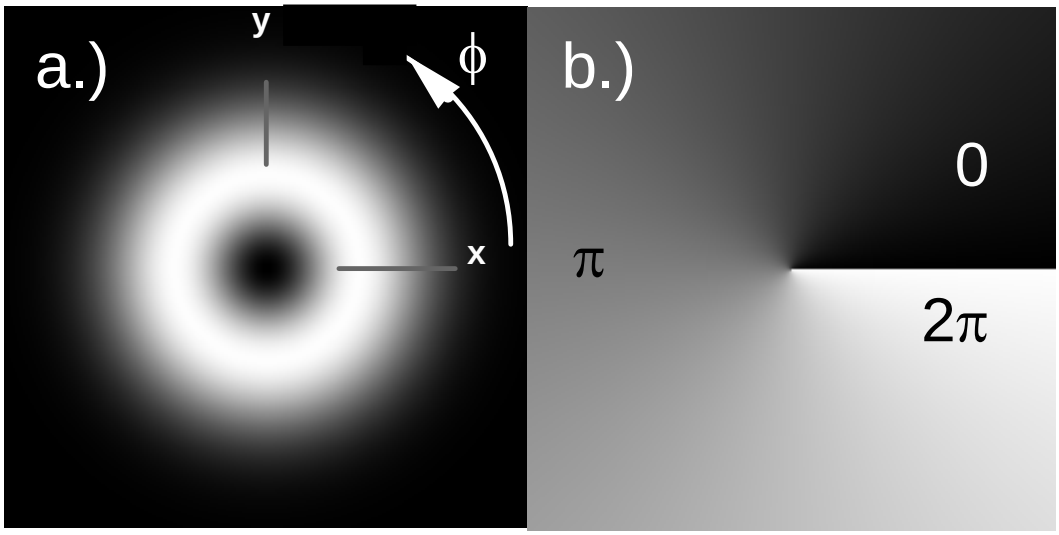

FIG. 1 The amplitude (a) and phase (b) profiles of an m=+1 optical vortex. At x=y=0 a dark null of destructive interference known as the vortex core forms at a phase singularity. The phase varies from 0-2π radians in a single revolution about the vortex core.

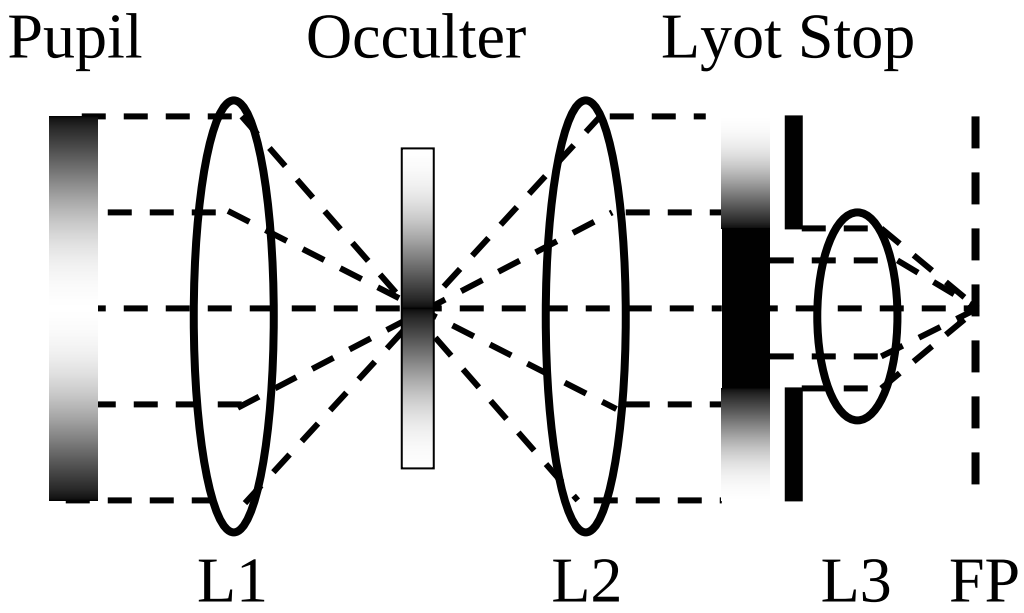

FIG. 2 A simple unfolded model of an optical vortex coronagraph. Lens (L1) represents the telescope optics, which focus the light from the entrance pupil onto the occulting mask, in our case an m=5 vortex phase mask. Lens (L2) collimates the light forming an exit pupil where a lyot stop is placed. A third lens (L3) re-images the light to the final image at (FP).

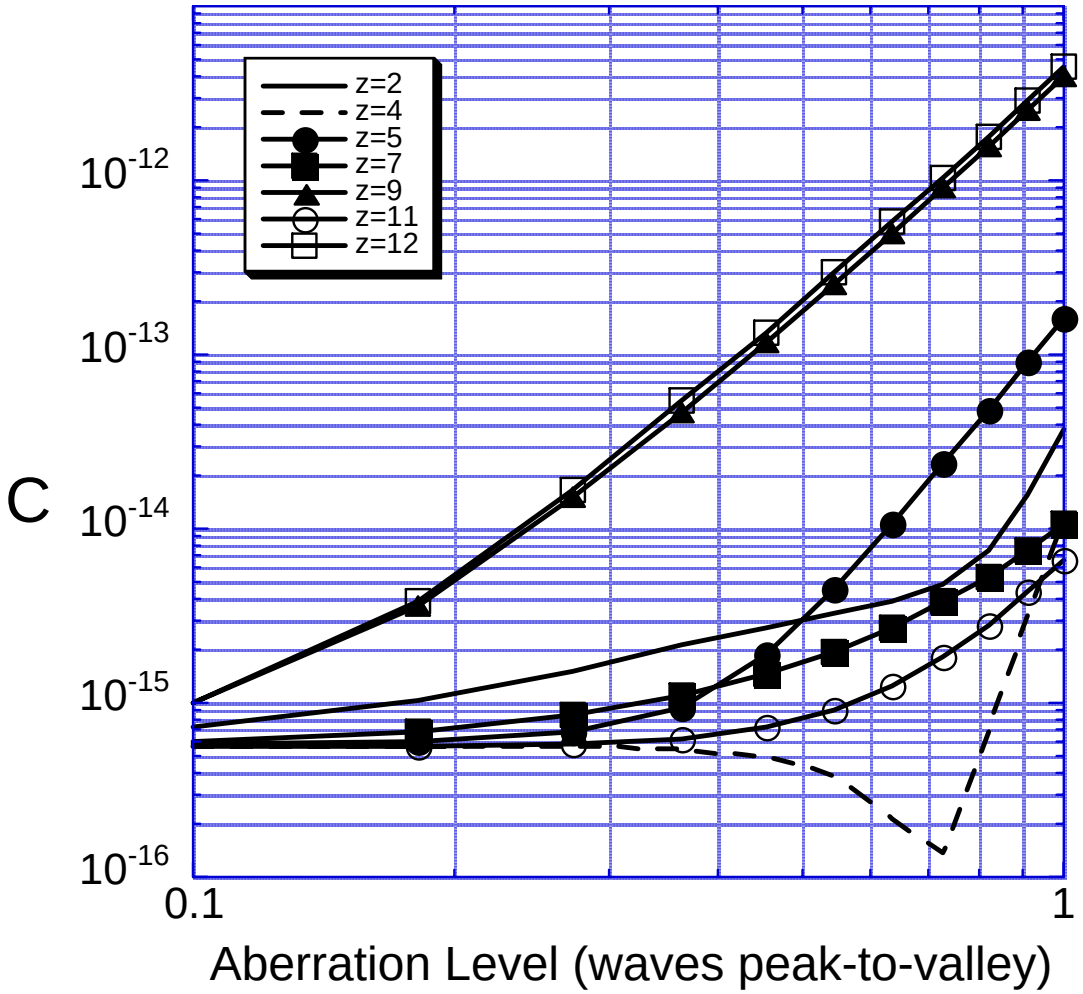

FIG. 3 Plots of Contrast vs. Aberration Level (waves peak-to-valley) depicting the aberration sensitivity of an m=5 vortex coronagraph to low-order Zernike modes (z=2-12). Only one of each of Tip/Tilt, astigmatism, coma, and trefoil, are shown since their curves were nearly identical.

Mode #	8^{th} order mask	m=5 vortex mask
2	8	9
3	8	9
4	4	--
5	4	6
6	4	6
7	4	4
8	4	4
9	4	5
10	4	5
11	2	5
12	2	5

TABLE. 1 A comparison of the aberration sensitivity to the low-order Zernike Modes for an 8^{th} order mask and an m=5 vortex coronagraph. Note: There is no tabulated value for focus (z=4) for the vortex case because an accurate estimate could not be obtained from the irregular plot depicted in Fig. 3.